Journal of Robotics and Control (JRC)
Volume 6, Issue 3, 2025
ISSN: 2715-5072, DOI: 10.18196/jrc.v6i3.26646

Balanced Linear Quadratic Gaussian Model Reduction for Islanded Microgrid Control Applications

Quoc-Xuyen Hoang [1], Hoang-Nha Phi [2], Minh-Cuong Nguyen [3*]
[1, 2] Faculty of Electrical Engineering, School of Electrical and Electronic Engineering, Hanoi University of Industry, Hanoi, Vietnam
[3] Faculty of Electrical Engineering, Thai Nguyen University of Technology, Thai Nguyen City, Vietnam
Email: [1] xuyen_hq@haui.edu.vn, [2] nhaph@haui.edu.vn, [3] nmc.etali@tnut.edu.vn
*Corresponding Author

***Abstract*—This study addresses the challenge of reducing the dynamic order of islanded microgrid (ISMG) systems, which are increasingly deployed to enhance power system stability and facilitate the integration of distributed energy resources such as photovoltaic arrays and battery storage. The main objective is to alleviate the computational complexities associated with high-order dynamic models in real-world microgrid control and optimization, thereby enabling more efficient and reliable controller design for practical applications. The contribution of this research is the development and implementation of a Balanced Linear-Quadratic Gaussian Model Reduction (BLQGMR) approach, which systematically integrates LQG control theory with state-space balancing techniques to generate reduced-order models that preserve essential controllability and observability properties. The BLQGMR method involves solving coupled Riccati equations to quantify the importance of system states, followed by a balanced truncation process that eliminates states with negligible influence on system input–output behavior. Numerical experiments on a representative ninth-order ISMG model demonstrate that the BLQGMR algorithm can effectively reduce the system order to between one and eight, with rigorous performance evaluation based on H_∞ and H_2 error norms. Results show that fourth- and fifth-order reduced models achieve a favorable trade-off between model accuracy and computational efficiency, with H_∞ errors of approximately 6.90×10^{-1} and 1.99×10^{-1}, and H_2 errors of 1.53×10^{-1} and 5.28×10^{-2}, respectively. These reduced models successfully reproduce the dynamic response of the original system across both time and frequency domains, as evidenced by Nyquist, Nichols, and step response analyses. The research demonstrates that BLQGMR provides a robust and practical solution for order reduction in ISMGs, supporting advanced control strategies while significantly reducing computational costs. Opening avenues to extend the approach to nonlinear and multivariable systems, as well as to address high-frequency limitations and cybersecurity challenges in intelligent microgrid control.**

Keywords*—Islanded Microgrid; Model Order Reduction; Power System Stability; Distributed Energy Resources; Balanced Linear-Quadratic Gaussian.

I. INTRODUCTION

The evolution of modern power systems has witnessed a paradigm shift toward decentralized architectures, with islanded microgrids (ISMGs) emerging as a pivotal solution for enhancing energy resilience, sustainability, and autonomy in both urban and remote contexts [1], [2], [3]. ISMGs, characterized by their capability to operate independently from the main grid, integrate a diverse array of distributed energy resources (DERs), including photovoltaic modules, wind turbines, and battery energy storage systems [4], [5], [6]. This architecture not only enables uninterrupted power supply under grid disturbances but also supports the global agenda for clean energy transition and carbon footprint reduction [7], [8], [9]. The deployment of ISMGs has been extensively studied for its potential to improve energy access, particularly in isolated regions where conventional grid extension is economically or technically unfeasible [10], [11], [12]. Furthermore, ISMGs facilitate the seamless integration of renewable energy, thereby enhancing grid flexibility and contributing to the mitigation of climate change impacts [13], [14], [15].

Despite these advantages, the operation and control of ISMGs present formidable technical challenges. The increasing penetration of intermittent renewables introduces significant dynamic uncertainties, nonlinearity, and variability in both generation and load profiles [16], [17], [18]. Accurate modeling of ISMGs must therefore account for stochastic fluctuations, unmodeled dynamics, and complex interactions among heterogeneous DERs [19], [20], [21]. Traditional control strategies, while effective under certain conditions, often fail to guarantee stability and optimality in the presence of high-dimensional state spaces and rapidly changing operating environments [22], [23], [24]. Moreover, the computational burden associated with high-order models can impede real-time control implementation, particularly as the number of controllable devices and system states increases [25], [26], [27]. These factors necessitate the development of advanced modeling, reduction, and control methodologies tailored to the unique characteristics of ISMGs [28], [29], [30].

Model order reduction (MOR) has become a cornerstone in addressing the computational and analytical complexity of modern power systems [31], [32], [33]. By simplifying high-order models while retaining essential input–output behaviors, MOR techniques enable efficient controller design, facilitate real-time simulation, and support robust system analysis [34], [35], [36]. While classical MOR methods such as balanced truncation, Hankel norm approximation, and Krylov subspace approaches have proven

effective for conventional power networks [37], [38], [39], their application to ISMGs is often restricted by challenges in handling unstable or nonlinear systems, and in ensuring that the reduced models retain the stability properties of the original system [40], [41], [42]. Recent advances in data-driven, machine learning-based, and hybrid MOR frameworks have shown promise in overcoming some of these limitations, yet they introduce new challenges related to data requirements, interpretability, and computational overhead [43], [44], [45]. Comparative studies highlight the need for MOR algorithms that achieve a careful balance between model simplicity, accuracy, and robustness, particularly under the nonstationary and uncertain conditions characteristic of ISMGs [46], [47], [48].

The Balanced Linear-Quadratic Gaussian Model Reduction (BLQGMR) algorithm represents a significant advancement in MOR for complex energy systems [49], [50], [51]. By enhancing balanced truncation based on LQG controller design, BLQGMR systematically identifies and retains the most influential system states, thereby ensuring that the reduced-order model preserves critical dynamic characteristics such as controllability, observability, and stability, retains the dominant (high-energy) singular values of the original system, and enables direct order reduction for unstable systems [52], [53], [54]. In the context of ISMGs, BLQGMR offers the potential to streamline controller design, reduce computational costs, and improve real-time responsiveness without sacrificing essential system performance [55], [56], [57]. However, the practical application of BLQGMR typically relies on the assumptions of linearity and time-invariance, assumptions that are often violated in real-world ISMGs due to nonlinearities, time-varying parameters, and stochastic disturbances introduced by renewable energy sources and variable loads [58], [59], [60]. Nevertheless, BLQGMR can still be effectively utilized by linearizing the system and considering its behavior at critical sampling instants, thus allowing for the preservation of essential dynamics even under practical operating conditions [61], [62], [63].

A comprehensive assessment of BLQGMR further reveals important trade-offs. While the algorithm effectively reduces system dimensionality and computational burden, it may also induce sensitivity to model uncertainties and potential loss of critical system dynamics in truncated states [64], [65], [66]. The impact of model reduction on transient response, stability margins, and robustness under extreme operating scenarios requires rigorous empirical validation and systematic sensitivity analysis [67], [68], [69]. Moreover, the interplay between reduction-induced simplifications and the real-time adaptability of ISMG controllers remains an open research question [70], [71], [72]. Comparative benchmarks with alternative MOR techniques, both classical and modern, are essential for elucidating the relative advantages and limitations of BLQGMR in practical ISMG applications [73], [74], [75]. Notably, the integration of BLQGMR with emerging technologies, such as artificial intelligence, self-adaptive control, and real-time data-driven optimization, has demonstrated potential for further enhancing the flexibility and resilience of microgrid operations [76], [77], [78]. However, these hybrid approaches also raise new challenges regarding interpretability, computational scalability, and standardization [79], [80], [81], [82].

In this study, we restrict the application of BLQGMR to high-order ISMG models that have been linearized and represented as linear time-invariant (LTI) dynamical systems. The main contributions of this research are as follows: (1) providing a rigorous theoretical analysis of BLQGMR's applicability to ISMGs, including explicit discussion of its underlying assumptions and practical limitations; (2) conducting comprehensive simulation-based validation and sensitivity analysis to assess the algorithm's performance in reducing the original 9th-order ISMG model to lower-order representations; and (3) focusing on generating reduced-order models, which are systematically compared to the original high-order system to offer practical guidance for users in selecting suitable lower-order representations as alternatives to more complex models.

To verify the model reduction capability of the BLQGMR algorithm, the authors applied this technique to the ISMG model [83] with the objective of simplifying the model, reducing computational complexity, and preserving the system's key dynamic characteristics, thereby enhancing reliability and stability during control. This research opens new avenues for intelligent control solutions, thereby promoting the development of islanded microgrids in the context of increasing integration of renewable energy.

II. BALANCED LINEAR-QUADRATIC GAUSSIAN MODEL REDUCTION (BLQGMR) ALGORITHM

Balanced LQG Model Reduction (BLQGMR) is an effective method for reducing the order of linear control systems, particularly in applications such as the stabilization of stratified flows based on linearized Navier–Stokes equations. This method integrates the Linear Quadratic Gaussian (LQG) control theory with balanced model reduction techniques and truncation, thereby generating a lower-order model that retains the system's vital input–output characteristics. The technique is described as follows [78]:

Input: The algorithm requires the fundamental system matrices E, K, F, and G, which correspond respectively to the mass matrix, state matrix, control matrix, and observation matrix of the system.

– Step 1: Solve the two Riccati equations (1) and (2).

$$K^T P_c E + E^T P_c K + G^T G - E^T P_c F F^T P_c E = 0 \quad (1)$$

$$K P_o E^T + E P_o K^T + F F^T - E P_o G^T G P_o E^T = 0 \quad (2)$$

– Step 2: Determine the LQG characteristic values as given in (3).

$$\begin{gathered} M = P_c E P_o \\ M v_i = \lambda_i v_i, \quad i = 1,2,\dots,n \end{gathered} \quad (3)$$

where $\lambda_i \geq 0$ are the LQG characteristic values indicating the relative importance of the states in terms of controllability and observability.

– Step 3: Apply a basis transformation to bring the system into a balanced LQG form, arranging the states in descending order of their characteristic values.

- Perform a Cholesky factorization as in (4).

$$P_c = UU^T;\ P_o = LL^T \tag{4}$$

where $U, L \in \mathbb{R}^{n\times n}$ are lower triangular matrices.

- Conduct a singular value decomposition (SVD) as in (5).

$$A = U^T EL; A = Z\Sigma Y^T \tag{5}$$

with $Z, Y \in \mathbb{R}^{n\times n}$ being orthogonal matrices satisfying $Z^T Z = I; Y^T Y = I;\ \Sigma = \text{diag}(\sigma_1, \sigma_2, \dots, \sigma_n)$ with $\sigma_1 \geq \sigma_2 \geq \cdots \geq \sigma_n \geq 0$ representing the singular values, where $\sigma_i = \sqrt{\lambda_i}$.

- Compute the transformation matrices as in (6).

$$W = LY\Sigma^{-1/2};\ V = UZ\Sigma^{-1/2} \tag{6}$$

where $\Sigma^{-1/2} = \text{diag}(\sigma_1^{-1/2}, \sigma_2^{-1/2}, \dots, \sigma_n^{-1/2}$

- Verify the balancing condition as in (7).

$$\begin{gathered} W^T EV = (LY\Sigma^{-\frac{1}{2}})^T E(UZ\Sigma^{-\frac{1}{2}}) \\ = \Sigma^{-1/2} Y^T L^T EUZ\Sigma^{-1/2} \\ L^T EU = (U^T EL)^T = (Z\Sigma Y^T)^T = Y\Sigma Z^T \end{gathered} \tag{7}$$

➔ $W^T EV = \Sigma^{-1/2} Y^T (Y\Sigma Z^T) Z\Sigma^{-1/2} = \Sigma^{-1/2}\Sigma\Sigma^{-1/2} = I$

- Compute the new matrices as (8), which $\tilde{P}_c = \tilde{P}_o = \Sigma$.

$$\begin{gathered} \tilde{E} = W^T EV = I, \quad \tilde{K} = W^T KV, \\ \tilde{F} = W^T F, \quad \tilde{G} = GV \end{gathered} \tag{8}$$

– Step 4: Eliminate the states whose characteristic values fall below a predefined threshold, thereby reducing the system's dimension.

- Establish the threshold and the reduction order: choose a threshold $\epsilon > 0$. Arrange the singular values σ_i in descending order and select the reduced order *r* such that $\sigma_1 \geq \sigma_2 \geq \cdots \geq \sigma_r > \epsilon, \quad \sigma_{r+1}, \dots, \sigma_n \leq \epsilon$.

  + Partition the matrix Σ as in (9).

$$\begin{gathered} \Sigma = \begin{bmatrix} \Sigma_r & 0 \\ 0 & \Sigma_{n-r} \end{bmatrix}; \\ \Sigma_r = \text{diag}(\sigma_1, \dots, \sigma_r); \Sigma_{n-r} = \text{diag}(\sigma_{r+1}, \dots, \sigma_n) \end{gathered} \tag{9}$$

- Partition the system matrices accordingly as in (10).

$$\tilde{K} = \begin{bmatrix} \tilde{K}_{11} & \tilde{K}_{12} \\ \tilde{K}_{21} & \tilde{K}_{22} \end{bmatrix}, \quad \tilde{F} = \begin{bmatrix} \tilde{F}_1 \\ \tilde{F}_2 \end{bmatrix}, \quad \tilde{G} = [\tilde{G}_1 \quad \tilde{G}_2] \tag{10}$$

where $\tilde{K}_{11} \in \mathbb{R}^{r\times r}, \tilde{K}_{12} \in \mathbb{R}^{r\times(n-r)}, \tilde{K}_{21} \in \mathbb{R}^{(n-r)\times r}, \tilde{K}_{22} \in \mathbb{R}^{(n-r)\times(n-r)}$; $\tilde{F}_1 \in \mathbb{R}^{r\times m}, \tilde{F}_2 \in \mathbb{R}^{(n-r)\times m}$; $\tilde{G}_1 \in \mathbb{R}^{p\times r}, \tilde{G}_2 \in \mathbb{R}^{p\times(n-r)}$.

- Discard the unimportant states and retain the components corresponding to Σ_r.

– Step 5: Construct the reduced-order model as in (11).

$$E_r = I_r; K_r = \tilde{K}_{11}; F_r = \tilde{F}_1; G_r = \tilde{G}_1 \tag{11}$$

Output: A reduced-order system with matrices E_r, K_r, F_r, G_r that maintain the stability characteristics of the original system, making it suitable for subsequent controller design in practical applications.

While BLQGMR offers a mathematically rigorous framework for reducing the order of linear control systems, its practical implementation in large-scale, high-dimensional systems such as ISMGs presents several nontrivial challenges. We analyze these limitations in detail and outline strategies to address them, thereby strengthening the applicability and reliability of the method:

– The core of BLQGMR involves solving two coupled algebraic Riccati equations, which, for a system of order *n*, typically require ($\mathcal{O}(n^3)$ operations per iteration using standard algorithms. For ISMGs, where *n* can be large due to detailed modeling of distributed energy resources and network dynamics, this computational burden may become prohibitive, especially for real-time or iterative design scenarios. To mitigate this, several approaches can be considered:

– Many practical ISMG models yield sparse or structured system matrices (e.g., block-diagonal, banded). Leveraging specialized numerical solvers that exploit such structures can significantly reduce both memory and computational requirements.

– Recent advances in iterative Riccati solvers, such as Krylov subspace methods and low-rank Cholesky factor ADI algorithms, enable efficient approximation of solutions for large-scale systems while maintaining accuracy.

– For very large systems, parallel algorithms and high-performance computing resources can be employed to accelerate Riccati equation solutions, making the method more tractable for practical ISMG applications.

BLQGMR, in its classical form, presumes that the underlying system is both linear and time-invariant (LTI). However, ISMGs inherently exhibit nonlinear behaviors and time-varying characteristics due to renewable energy fluctuations, load dynamics, and converter nonlinearities. To bridge this gap:

– The method can be applied to locally linearized models around operating points of interest. However, the validity of such linear approximations must be assessed, particularly under large disturbances or rapid parameter shifts.

– Constructing a set of linearized models at representative operating conditions and performing model reduction for each can improve coverage of the nonlinear operating envelope.

– Emerging research on model reduction for linear parameter-varying and nonlinear systems, such as empirical Gramians and Carleman linearization, may offer pathways to generalize BLQGMR beyond the LTI paradigm.

– The process of truncating states based on LQG characteristic values σ_i assumes that states with smaller values are always negligible. However, in practice, states deemed unimportant under nominal conditions may become critical during transients or under parameter uncertainty. To address this:

- Prior to truncation, conducting a sensitivity analysis of system performance with respect to each state can reveal hidden vulnerabilities and guide more informed state selection.
- Instead of a fixed threshold ϵ, employing adaptive or system-dependent criteria, such as energy contribution, frequency response impact, or robustness margins, can enhance the reliability of the reduction process.
- After reduction, rigorous robustness analysis, including worst-case and probabilistic scenarios, should be performed to ensure that essential dynamics are preserved, especially under disturbances and uncertainties.

– The simplified representation of each ISMG component as a first-order transfer function, while analytically convenient, may inadequately capture the complex, nonlinear, and stochastic behaviors of real-world devices such as photovoltaic inverters, wind turbines, and storage systems. This oversimplification can compromise the predictive fidelity of both the full-order and reduced-order models. To improve model realism:

- Employ higher-order or nonlinear models for key components, validated against detailed simulations or experimental data.
- The overall system model should explicitly account for coupling between AC/DC converters, heterogeneous loads, and network interconnections, as such interactions are pivotal for accurate dynamic behavior.
- The accuracy of the linearized and reduced models should be systematically validated by comparing their responses to those of high-fidelity nonlinear models under a range of realistic operating scenarios.

– The integration of BLQGMR with simplified ISMG models must be accompanied by a thorough evaluation of robustness, particularly in the face of abrupt load changes, renewable intermittency, and parameter variations. This includes:

- Performing extensive simulations under stochastic and worst-case scenarios to assess the stability and performance of the reduced-order model.
- Investigating the impact of model reduction on adaptive and robust controller designs, ensuring that the reduced model remains suitable for real-time control tasks.
- Experimental studies or hardware-in-the-loop simulations should be conducted to confirm the practical reliability of the reduced-order models and associated controllers.

III. ARCHITECTURE AND DYNAMIC MODELING OF THE ISLANDED MICROGRID

An Islanded Microgrid (ISMG) is a localized power system that can operate independently from the main grid. Its overall architecture, as illustrated in Fig. 1, comprises several key components [83]:

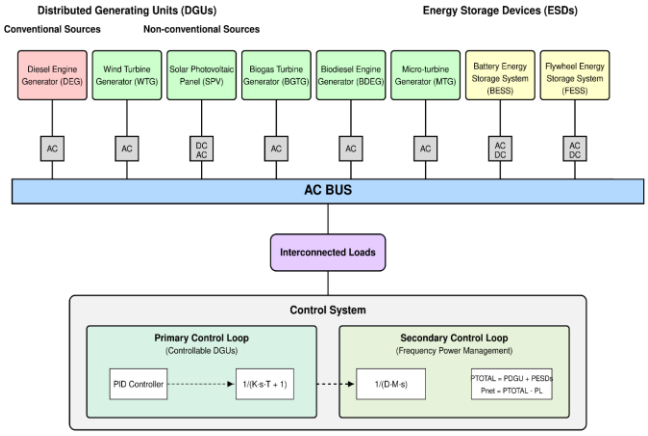

Fig. 1. Block Diagram of the ISMG System

1. Distributed Generating Units (DGUs):
   – Diesel Engine Generator (DEG).
   – Non-conventional sources:
   + Wind Turbine Generator (WTG).
   + Solar Photovoltaic Panel (SPV).
   + Biogas Turbine Generator (BGTG).
   + Biodiesel Engine Generator (BDEG).
   + Micro Turbine Generator (MTG).
2. Energy Storage Devices (ESDs)
   – Battery Energy Storage System (BESS).
   – Flywheel Energy Storage System (FESS).
   – Electric Vehicle (EV).
   – Aqua Electrolyzer (AE).
   – Fuel Cell (FC).
3. Interconnected Loads: These loads may be either DC or AC.
4. Power Converters: DC/AC, AC/DC, and DC/DC converters are employed.
5. Control System: This consists of two main control loops:

– Primary Control Loop: Directly regulates the controllable DGUs using a PID controller; the functional blocks are modeled as first-order transfer functions.

– Secondary Control Loop: Manages the overall system frequency and power, coordinating the power flow

among various components to respond to load and source fluctuations.

The modeling process of the ISMG system begins with determining the individual transfer functions of its components to obtain an overall system transfer function. Typically, the transfer function of each component is expressed in the form $\mathcal{T}_i(\rho) = \frac{\alpha_i}{1+\rho\beta_i}$ where α_i represents the amplification factor of the ith component and β_i denotes the time constant characteristic of its dynamic process. Specifically, the components are modeled as follows [83]:

– The transfer function of the DEG block is given in (11).

$$\mathcal{T}_{\text{DEG}}(s) = \frac{\alpha_d}{1+s\beta_d};\ \alpha_d = K_{deg},\ \beta_d = T_{deg} \tag{11}$$

– The transfer function of the SPV block is in (12).

$$\mathcal{T}_{\text{SPV}}(s) = \frac{\alpha_s}{1+s\beta_s};\quad \alpha_s = K_{spv},\ \beta_s = T_{spv} \tag{12}$$

– The transfer function of the WTG block is in (13).

$$\mathcal{T}_{\text{WTG}}(s) = \frac{\alpha_w}{1+s\beta_w};\quad \alpha_w = K_{wt},\ \beta_w = T_{wt} \tag{13}$$

– The transfer function of the BGTG block is approximated in (14).

$$\mathcal{T}_{\text{BGTG}}(s) \approx \frac{\alpha_b}{1+s\beta_b};\quad \alpha_b = K_{bgtg},\ \beta_b = T_{bgtg} \tag{14}$$

– The transfer function of the BDEG block is approximated in (15).

$$\mathcal{T}_{\text{BDEG}}(s) \approx \frac{\alpha_{bd}}{1+s\beta_{bd}};\quad \alpha_{bd} = K_{bdeg},\ \beta_{bd} = T_{bdeg} \tag{15}$$

– The transfer function of the MTG block is given in (16).

$$\mathcal{T}_{\text{MT}}(s) = \frac{\alpha_m}{1+s\beta_m};\quad \alpha_m = K_{mt},\ \beta_m = T_{mt} \tag{16}$$

– The transfer function of the AE-FC block is in (17).

$$\mathcal{T}_{\text{AE-FC}}(s) = \frac{\alpha_{ae}}{1+s\beta_{ae}};\quad \alpha_{ae} = K_{ae-fc},\ \beta_{ae} = T_{ae-fc} \tag{17}$$

– The transfer function of the BESS block is given in (18).

$$\mathcal{T}_{\text{BESS}}(s) = \frac{\alpha_{be}}{1+s\beta_{be}};\quad \alpha_{be} = K_{bess},\ \beta_{be} = T_{bess} \tag{18}$$

– The transfer function of the FESS block is in (19).

$$\mathcal{T}_{\text{FESS}}(s) = \frac{\alpha_f}{1+s\beta_f};\quad \alpha_f = K_{fess},\ \beta_f = T_{fess} \tag{19}$$

– The transfer function of the EV block is given in (20).

$$\mathcal{T}_{\text{EV}}(s) = \frac{\alpha_{ev}}{1+s\beta_{ev}};\quad \alpha_{ev} = K_{ev},\ \beta_{ev} = T_{ev} \tag{20}$$

– The dynamics of the generator are modeled as in (21).

$$\mathcal{T}_{\text{GD}}(\rho) = \frac{1}{\gamma + s\delta} \tag{21}$$

where γ, δ correspond to the damping coefficient and stiffness of the system, respectively.

The interconnection of the individual transfer functions of these components yields the overall system transfer function, which is expressed in (22) as:

$$(s) = \frac{\Delta\varphi(s)}{\Delta\Pi(s)} = \frac{\sum_{i=0}^{7} a_i\, s^i}{\sum_{j=0}^{9} b_j\, s^j} \tag{22}$$

where $\Delta\varphi(s)$ represents the frequency error and $\Delta\Pi(s)$ represents the net power error. By substituting the appropriate values into (22), the full-order transfer function of the ISMG is obtained as a ninth-order model, as in (23).

$$H(s) = \frac{\begin{array}{c}3.003 + 16.67s + 34.58s^2 \\ +33.32s^3 + 15.03s^4 + 2.832s^5 \\ +0.2324s^6 + 0.00694s^7\end{array}}{\begin{array}{c}0.0587 + 4.882s + 16.19s^2 \\ +27.32s^3 + 24.86s^4 + 12.13s^5 \\ +3.147s^6 + 0.44s^7 + 0.0312s^8 \\ +0.00087s^9\end{array}} \tag{23}$$

IV. Model Reduction of the ISMG System Using the BLQGMR Algorithm

The BLQGMR algorithm was implemented in MATLAB to reduce the order of the 9th-order ISMG system, as described by the mathematical model in equation (23), down to a first-order system. The resulting approximation errors are presented in Table I, with corresponding graphical representations shown in Fig. 2.

TABLE I. H_∞ and H_2 Norm Errors of the Reduced-Order Models for ISMG using BLQGMR

Reduced Order	H_∞ Error Norm	H_2 Error Norm
1	1.366285×10^{1}	6.898688×10^{-1}
2	1.106420×10^{0}	3.292628×10^{-1}
3	2.883516×10^{0}	5.813126×10^{-1}
4	6.900646×10^{-1}	1.532748×10^{-1}
5	1.986987×10^{-1}	5.283805×10^{-2}
6	1.126398×10^{-2}	2.270563×10^{-2}
7	1.133995×10^{-3}	3.030480×10^{-4}
8	4.666255×10^{-5}	9.903603×10^{-6}

From the data in Table I and Fig. 2, it is evident that the H_∞ norm error quantifies the maximum deviation between the original and reduced models across the entire frequency spectrum, while the H_2 norm error reflects the average energy

discrepancy, emphasizing the dynamic signal energy effects. As the reduced order increases from 1 to 8, both error metrics exhibit a significant decline, particularly for r ≥ 6, where the errors become negligibly small. This indicates that the BLQGMR algorithm effectively preserves the dynamic characteristics of the original system even at lower orders, which is crucial for controller design in ISMG systems. It enables reduced computational complexity and time while maintaining dynamic responses closely aligned with the full-order model.

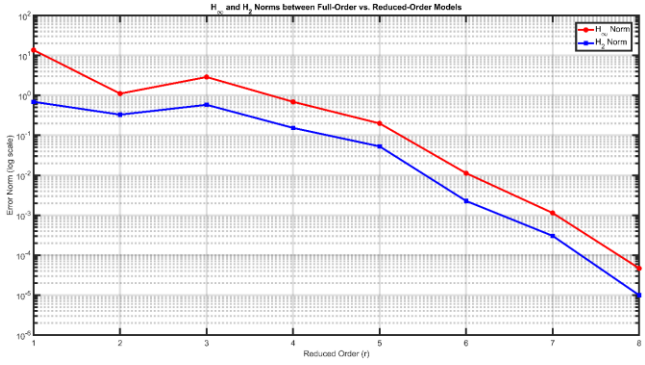

Fig. 2. Error plots of H_∞ and H_2 norms between the original system and reduced-order models for varying r

The selection of the reduced order is based on balancing several criteria: minimizing the reduced order as much as possible, keeping the model reduction error as low as possible, retaining as many of the original system's significant singular values as possible, and ensuring that the time-domain and frequency-domain input-output responses closely match those of the original system. Based on these criteria, and after multiple simulation trials, we selected reduced orders of 2, 4, and 5 for further analysis.

Selecting reduced orders of 2, 4, and 5, we obtain corresponding error analyses depicted through Nyquist plots, Nichols plots, phase error versus frequency, magnitude error versus frequency, and amplitude error over time, as illustrated in Fig. 3 through Fig. 7.

Fig. 3 demonstrates the discrepancies between the original model and lower-order models in the Nyquist plot. The model with r = 2 exhibits potential instability risks, as indicated by multiple loops near the critical point (-1, 0). The r = 4 model ensures better stability margins, and the r = 5 model outperforms the other two in terms of stability and accuracy.

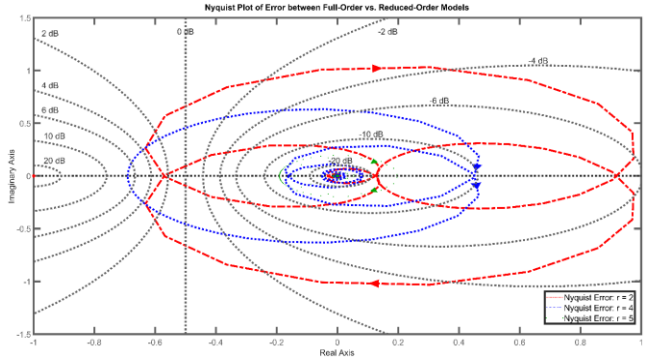

Fig. 3. Nyquist plot errors between the original model and reduced-order models

Fig. 4 depicts the error between the original model and the reduced-order models on the Nichols chart, where the vertical axis represents the open-loop gain ranging from -120 dB to 40 dB, and the horizontal axis denotes the open-loop phase spanning from 0 deg to 1980 deg. The model with order r = 5 exhibits a smaller error at high frequencies compared to models with r = 2 and r = 4, maintaining an open-loop gain close to 0 dB at higher phase values. The r = 4 model achieves a better balance of error across low and high frequencies, while the r = 5 model demonstrates stability across the entire frequency range.

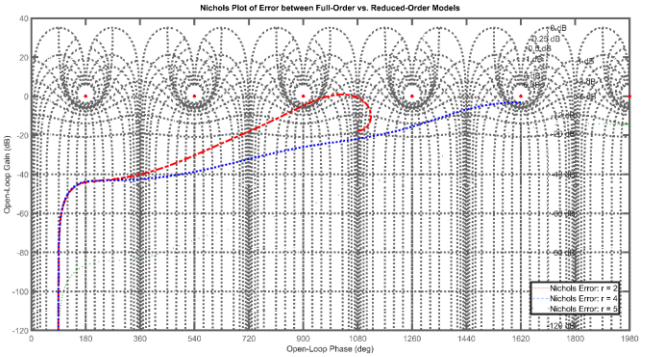

Fig. 4. Error between the original model and reduced-order models on the Nichols plot

Fig. 5 provides details on the magnitude error across a frequency range from 10^{-2} rad/s to 10^{2} rad/s, with errors varying between 10^{-7} and 10^{1}. For the r = 5 model, the error rarely exceeds 10^{-1}, indicating strong capability in reproducing the magnitude response. All three reduced models exhibit low errors at low frequencies; however, the error increases at higher frequencies, with the most pronounced increase observed for r = 2.

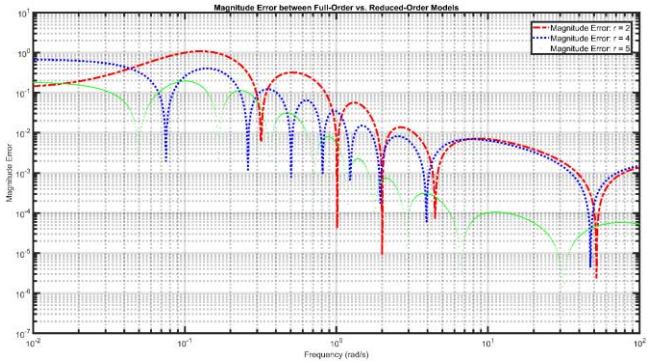

Fig. 5. Magnitude error between the original model and reduced-order models in the time domain

Fig. 6 presents the phase error between the original system and the reduced-order models over a frequency range from 10^{-2} rad/s to 10^{2} rad/s, with phase errors fluctuating between 10^{-5} and 10^{2} degrees. The phase error decreases as the model order increases, with the r = 5 model maintaining an error below 10^{0} degrees across most of the frequency range, reflecting high accuracy. Phase errors rise at high frequencies across all orders, with the effect being particularly significant for r = 2, potentially impacting frequency-sensitive applications.

Fig. 7 provides information on the step response error between the original model and the reduced-order models

over a time domain from 0 to 30 seconds, with absolute errors ranging from 10^{-7} to 10^{3}. The error decreases significantly from r = 2 to r = 5, with the r = 5 model achieving the smallest error, below 10^{-1}, in the steady state. Both the r = 4 and r = 5 models effectively reproduce the step response, particularly during the transient phase, outperforming the r = 2 model. The minor difference between r = 4 and r = 5 suggests that r = 4 offers a balanced trade-off between accuracy and complexity.

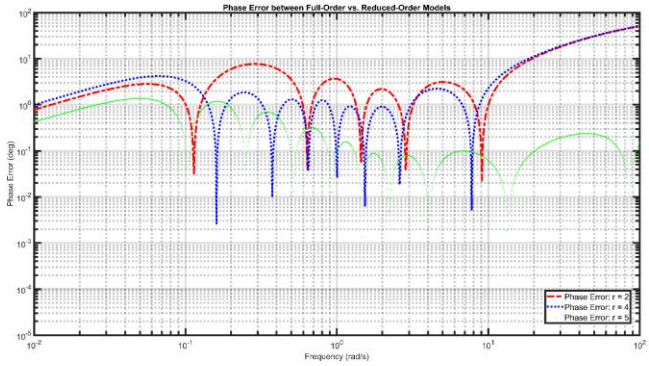

Fig. 6. Phase error between the original system and reduced-order models in the frequency domain

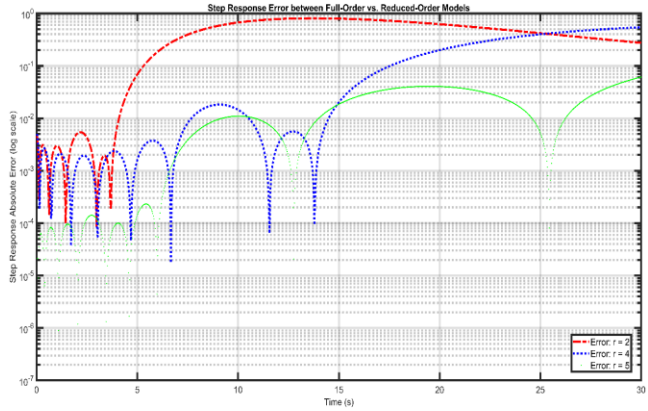

Fig. 7. Step response error between the original model and reduced-order models in the time domain

Analysis of the impulse response between the 9th-order original system and its reduced-order systems in Fig. 8 reveals that the 2nd-order reduced system closely approximates the original system for times less than 2 seconds. However, as time increases, the response of the 2nd-order system diverges from the original. In contrast, the 4th- and 5th-order systems closely track the original system's response across the simulated time domain, with the 5th-order system exhibiting the highest degree of alignment. Consequently, the 4th- or 5th-order systems are recommended as viable substitutes for the 9th-order original system in time-domain applications.

From the magnitude response across frequencies in Fig. 9, it is observed that the data lines corresponding to the reduced-order systems of orders 2, 4, and 5 closely align with that of the original system. Consequently, these reduced-order systems can be considered as viable substitutes for the original system in applications related to magnitude responses within the frequency domain.

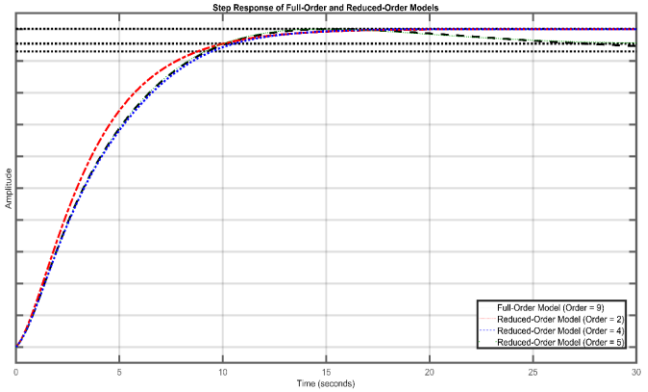

Fig. 8. Step response plot between the original system and reduced-order systems

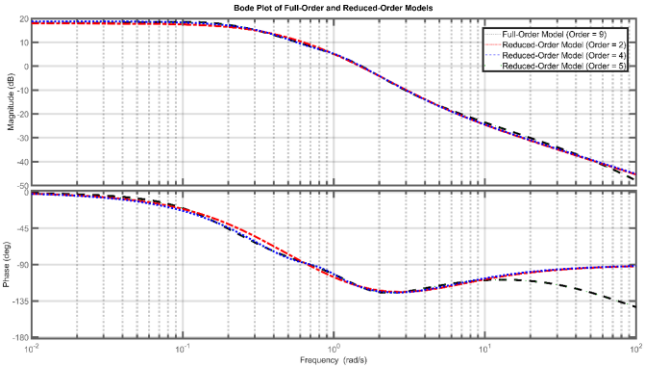

Fig. 9. Bode plot between the 9th-order original system and reduced-order systems

Regarding the phase response across frequencies, at frequencies below 10^{1} rad/s, the reduced-order systems effectively approximate the original system. Therefore, these reduced-order systems may be employed in lieu of the original system for applications involving phase responses in the low-frequency range below 10^{1} rad/s.

Analysis of the results reveals that the BLQGMR algorithm demonstrates effectiveness in reducing the order of the ISMG model, with accuracy improving as the reduced order increases from 2 to 5. Although the reduced-order models, particularly those of order 4 and 5, demonstrate strong performance in both steady-state and frequency-domain analyses, it is crucial to acknowledge the inherent limitations of lower-order reductions. Specifically, the second-order model exhibits potential stability risks, as indicated by Nyquist and Nichols analyses, which may compromise system robustness under practical operating conditions. Furthermore, while steady-state errors remain low, transient mismatches following abrupt disturbances—such as sudden load changes or rapid fluctuations in renewable generation—can significantly impact ISMG stability. High-frequency discrepancies observed in Bode plots also warrant attention, especially for digital controllers operating over wide frequency bands. Therefore, the order selection for model reduction should reflect a careful balance between model simplicity, dynamic fidelity, and application-specific requirements, with fourth- and fifth-order models offering an optimal trade-off for most ISMG control scenarios.

The Monte Carlo study injected perturbed step inputs (step plus white-noise) into the full-order and three reduced-order models (r = 2, 4, 5) and computed the per-run root-mean-square (RMS) error between each reduced response and the full-order response over 100 trials. The results and their envelope plot in Table II and Fig. 10 (showing the 5th–95th percentile band and the mean error trajectory) reveal several key insights:

TABLE II. MONTE CARLO RMS ERROR STATISTICS FOR REDUCED-ORDER MODELS

Reduced Order	Mean RMS Error	Std. Dev. of RMS
2	0.53119	0.002155
4	0.23798	0.0010695
5	0.023353	0.00017876

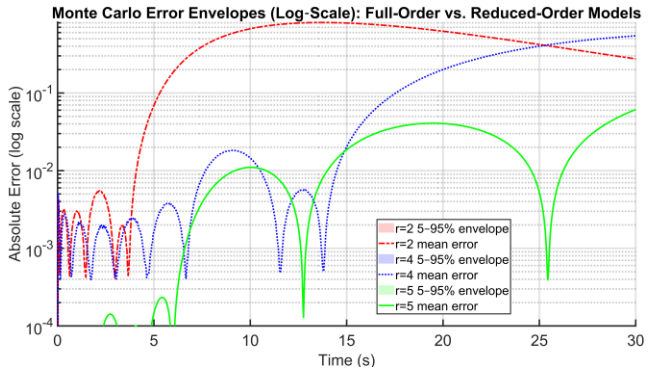

Fig. 10. Monte Carlo Error Envelopes on Logarithmic Scale for Full-Order versus Reduced-Order Models

– Quantitative accuracy analysis reveals that the second-order reduced model (r = 2) exhibits a relatively high average RMS error of approximately 0.53, indicating substantial deviation from the full-order system under random disturbances. Increasing the order to r = 4 reduces the mean RMS error to about 0.238, effectively halving the error and significantly improving fidelity. Notably, the fifth-order model (r = 5) achieves a much lower error of around 0.023, demonstrating that adding just one additional state beyond r = 4 yields a dramatic enhancement in accuracy.

– The error dynamics, as illustrated by the envelope plots, show that for r = 2 (red line), the 5–95% envelope expands rapidly after 5 seconds, peaking near 0.8 at 15 seconds, with the mean error closely following the envelope's crest, reflecting significant and systematic deviation. For r = 4 (blue line), the envelope grows more gradually, reaching a peak around 0.3 by the end of the simulation, in line with its moderate RMS error. In contrast, the r = 5 (green line) model maintains both the 5–95% envelope and mean error below 0.05 throughout most of the 30-second window, demonstrating excellent tracking of the full-order system even in the presence of noise.

– The small standard deviations (all on the order of 10^{-3} or less) indicate that the RMS errors are very consistent across 100 Monte Carlo trials. In particular, r = 5 exhibits a remarkable tight distribution (std $\approx 1.8\times10^{-4}$), confirming that its performance is both accurate and reliable under random input perturbations.

– These results highlight a clear trade-off in model selection: while r = 2 achieves the greatest reduction in dimension, its high error makes it unsuitable for control applications. The r = 4 model offers a substantial reduction to four states with moderate error (~0.24 RMS), which may be acceptable for less demanding scenarios. However, r = 5 provides the optimal balance, reducing the system order from 9 to 5 while keeping the RMS error around 0.02 and maintaining an error envelope an order of magnitude lower than r = 4, making it highly appropriate for robust control design.

The Monte Carlo results confirm that the BLQGMR reduction to order 5 delivers excellent dynamic fidelity and robustness to input perturbations, with minimal variance across trials. Thus, for applications demanding both computational efficiency and high accuracy, the fifth-order model represents the optimal choice among the tested reductions.

V. CONCLUSION

This study systematically applied the Balanced Linear Quadratic Gaussian Model Reduction (BLQGMR) algorithm to the order reduction of islanded microgrid (ISMG) models, with a focus on preserving the essential controllability and observability properties intrinsic to the original system. Through rigorous evaluation using both H_∞ and H_2 norm-based error metrics, we demonstrated that reduced-order models, especially those of orders r = 4 and r = 5, achieve a favorable compromise between complexity reduction and dynamic fidelity. The results indicate that as the retained order increases, the approximation errors decrease, confirming that BLQGMR can effectively capture the critical dynamics necessary for reliable control design while substantially simplifying the mathematical representation.

Nevertheless, certain methodological limitations warrant further attention. The BLQGMR approach, as implemented here, operates under the assumptions of linearity and time-invariance, which may not fully encompass the nonlinearities and time-varying characteristics common in practical microgrid operation, such as those introduced by renewable energy sources and fluctuating loads. While the reduced-order models perform well in replicating nominal system dynamics, their robustness in the presence of substantial parameter variations, unmodeled dynamics, or external disturbances remains an open question and should be systematically investigated in future work. Although this study provides a detailed analysis of the BLQGMR algorithm at various reduced orders, it does not include direct quantitative comparisons with alternative model reduction techniques. As such, future research should incorporate benchmarking against other established methods, such as proper orthogonal decomposition, moment-matching, or data-driven approaches, to more comprehensively evaluate the relative strengths and limitations of BLQGMR within the context of microgrid applications. From a practical standpoint, the reduced-order models derived via BLQGMR offer significant potential to enhance the computational efficiency of controller synthesis and optimization for ISMGs. This efficiency is particularly relevant for real-time applications where computational resources and response

times are critical. However, further validation in hardware-in-the-loop or experimental settings would be valuable to confirm the practical utility and reliability of these models under realistic operating conditions.

Looking ahead, several research directions emerge as particularly promising. Extending the BLQGMR framework to accommodate nonlinear and time-varying systems, potentially by integrating recent advances in nonlinear model reduction or adaptive control, would enhance its applicability to modern, complex microgrid architectures. Additionally, the integration of advanced optimization techniques to refine reduction parameters, possibly leveraging data-driven or machine learning-based strategies, could further improve model accuracy and robustness. Finally, as intelligent control systems become increasingly prevalent in smart grid environments, it is crucial to systematically assess the cybersecurity implications of model reduction, particularly regarding the resilience of reduced-order controllers to malicious attacks or system faults.

In summary, this work advances the field of microgrid control by providing a rigorous assessment of the BLQGMR algorithm's capabilities for model order reduction. The findings contribute foundational insights that inform the development of efficient, robust, and secure control strategies for future smart grid applications.

FUNDING

This research received no external funding.

ACKNOWLEDGMENT

The authors gratefully acknowledge Thai Nguyen University of Technology, Vietnam, for supporting this work.

REFERENCES

[1] R. Jafari, B. F. Yancey, S. Bye, G. Yakle, and A. Meissner, "Utility-Scale BESS/PV Microgrid Islanding Challenges And Protection Considerations," in *2024 IEEE Power & Energy Society General Meeting (PESGM)*, pp. 1-5, 2024.

[2] R. Chaudhary, V. P. Singh, A. Mathur, U. K. Yadav, A. V. Waghmare, and K. Murari, "Differentiation Method Based Approximation of Higher Order Islanded Microgrid System," in *2024 IEEE 4th International Conference on Sustainable Energy and Future Electric Transportation (SEFET)*, pp. 1-6, 2024.

[3] S. Manikandan, "Higher Order Sliding Mode Controls For The Voltage Control Of Microgrids," in *2022 IEEE 19th India Council International Conference (INDICON)*, pp. 1-6, 2022.

[4] N. A. Sârbu and D. Petreuș, "Model Development for an Islanded Microgrid," in *2023 46th International Spring Seminar on Electronics Technology (ISSE)*, pp. 1-6, 2023.

[5] M. Talaat, M. H. Elkholy, A. Alblawi, and T. Said, "Artificial intelligence applications for microgrids integration and management of hybrid renewable energy sources," *Artificial Intelligence Review*, vol. 56, no. 9, pp. 10557-10611, 2023.

[6] S. Murugesan, "A hybrid unintentional islanding identification methodology for iidgs," *IEEE Transactions on Industry Applications*, 2024.

[7] O. Bassey. *Control and Black Start Restoration of Islanded Microgrids*. Doctoral dissertation, 2020.

[8] Z. Wu, Y. Liu, P. Chen, and Y. Chen, "Economic operation of islanded micro-grids via modified active disturbance rejection control," *International Journal of Electrical Power & Energy Systems*, vol. 158, p. 109974, 2024.

[9] I. F. Davoudkhani, P. Zare, A. Y. Abdelaziz, M. Bajaj, and M. B. Tuka, "Robust load-frequency control of islanded urban microgrid using 1PD-3DOF-PID controller including mobile EV energy storage," *Scientific Reports*, vol. 14, no. 1, p. 13962, 2024.

[10] S. Yue, N. Xu, L. Zhang, and N. Zhao, "Observer-based event-triggered adaptive fuzzy hierarchical sliding mode fault-tolerant control for uncertain under-actuated nonlinear systems," *International Journal of Fuzzy Systems*, pp. 1-18, 2024.

[11] M. Vicente, A. Imperadore, F. X. Correia da Fonseca, M. Vieira, and J. Cândido, "Enhancing Islanded Power Systems: Microgrid Modeling and Evaluating System Benefits of Ocean Renewable Energy Integration," *Energies*, vol. 16, no. 22, p. 7517, 2023.

[12] A. Villalón, C. Muñoz, J. Muñoz, and M. Rivera, "Fixed-Switching-Frequency Modulated Model Predictive Control for Islanded AC Microgrid Applications," *Mathematics*, vol. 11, no. 3, p. 672, 2023.

[13] A. J. Handique, R. A. Peer, and J. Haas, "Understanding the Challenges for Modelling Islands' Energy Systems and How to Solve Them," *Current Sustainable/Renewable Energy Reports*, vol. 11, no. 4, pp. 95-104, 2024.

[14] P. Onu, A. Pradhan, and N. S. Madonsela, "Autonomous Microgrids Optimization Using Reinforcement Learning: Applications, Challenges and Prospects," in *2024 1st International Conference on Smart Energy Systems and Artificial Intelligence (SESAI)*, pp. 1-6, 2024.

[15] L. Vuić, J. Hivziefendić, M. Sarić, and J. Osmić, "Voltage and frequency control of solar–battery–diesel based islanded microgrid," *Journal of Electrical Engineering*, vol. 74, no. 6, pp. 442-453, 2023.

[16] E. Şehirli and Ö. Usta, "Grid Connected and Islanded Operation of Microgrids including SMES, SC, and Li/Ion Based PV Systems," in *2023 IEEE PES GTD International Conference and Exposition (GTD)*, pp. 398-403, 2023.

[17] M. A. Rios, S. Pérez-Londoño, and A. Garcés, "Dynamic performance evaluation of the secondary control in islanded microgrids considering frequency-dependent load models," *Energies*, vol. 15, no. 11, p. 3976, 2022.

[18] J. Duarte, M. Velasco, P. Martí, A. Camacho, J. Miret, and C. Alfaro, "Decoupled simultaneous complex power sharing and voltage regulation in islanded AC microgrids," *IEEE Transactions on Industrial Electronics*, vol. 70, no. 4, pp. 3888-3898, 2022.

[19] A. Khan, M. M. Khan, and J. Chuanwen, "Distributed optimization for microgrids control and management with virtual voltage source segregation," *Renewable Energy Focus*, vol. 2025, no. 100709, 2025.

[20] Q. L. Lam, D. Riu, and A. I. Bratcu, "Frequency Robust Control Application in Islanded Microgrids Considering Parametric Uncertainties and Distinct Photovoltaic Penetration Rate Scenarios," *IEEE Access*, vol. 11, pp. 92589-92616, 2023.

[21] M. Ramesh, A. K. Yadav, and P. K. Pathak, "Intelligent adaptive LFC via power flow management of integrated standalone micro-grid system," *ISA Transactions*, vol. 112, pp. 234-250, 2021.

[22] Y. Zheng, S. H. Yao, T. Wu, W. Hai, X. Zheng, and L. Xia, "Control Strategies for the PV-Integrated Islanded Microgrid Under Normal and Fault Conditions," in *Springer Science+Business Media*, pp. 422-436, 2024.

[23] J. Yang, C. K. Tse, and Y. Liu, "Nonlinear Behavior and Reduced-Order Models of Islanded Microgrid," *IEEE Transactions on Power Electronics*, vol. 37, pp. 9212-9225, 2022.

[24] X. Wang, R. A. Perez, B. Wainwright, Y. Wang, and M. P. Mignolet, "Nonintrusive Nonlinear Reduced Order Models for Structures in Large Deformations: Validations to Atypical Structures and Basis Construction Aspects," *Vibration*, vol. 5, no. 1, pp. 20-58, 2022.

[25] A. Afshari, M. Davari, M. Karrari, W. Gao, and F. Blaabjerg, "A Multivariable, Adaptive, Robust, Primary Control Enforcing Predetermined Dynamics of Interest in Islanded Microgrids Based on Grid-Forming Inverter-Based Resources," *IEEE Transactions on Automation Science and Engineering*, pp. 1-13, 2023.

[26] E. E. Pompodakis, G. D. Tinajero, and E. S. Karapidakis, "Modelling the steady-state of secondary control in islanded AC microgrids," *International Journal of Electrical Power & Energy Systems*, vol. 153, p. 109295, 2023.

[27] J. F. Huaman, L. E. dos Santos, J. C. U. Pena, J. A. Pomilio, and D. Dotta, "Seamless Transitions Between Grid-Tied and Islanded Operation in a Brazilian Microgrid," in *2024 IEEE Power & Energy Society General Meeting (PESGM)*, pp. 1-5, 2024.

[28] E. Szilagyi, D. Petreus, T. Patarau, and N. A. Sarbu, "Energy Management System for an Islanded Microgrid using Stochastic Dynamic Programming under Uncertainty," *2023 IEEE 29th International Symposium for Design and Technology in Electronic Packaging (SIITME)*, pp. 110-114, 2023.

[29] M. Hajihosseini, V. Lesic, H. I. Shaheen, and P. Karimaghaee, "Sliding Mode Controller for Parameter-Variable Load Sharing in Islanded AC Microgrid," *Energies*, vol. 15, no. 16, p. 6029, 2022.

[30] M. A. Taher, M. Tariq, and A. I. Sarwat, "Trust-based detection and mitigation of cyber attacks in distributed cooperative control of islanded AC microgrids," *Electronics*, vol. 13, no. 18, p. 3692, 2024.

[31] A. K. Hado, B. S. Bashar, M. M. Abdul Zahra, R. Alayi, Y. Ebazadeh, and I. Suwarno, "Investigating and Optimizing the Operation of Microgrids with Intelligent Algorithms," *Journal of Robotics and Control (JRC)*, vol. 3, no. 3, pp. 279-288, 2022.

[32] D. Murugesan, K. Jagatheesan, P. Shah, and R. Sekhar, "Optimization of load frequency control gain parameters for stochastic microgrid power system," *Journal of Robotics and Control (JRC)*, vol. 4, no. 5, pp. 726-742, 2023.

[33] M. Zadehbagheri, A. Ma'arif, R. Ildarabadi, M. Ansarifard, and I. Suwarno, "Design of multivariate PID controller for power networks using GEA and PSO," *Journal of Robotics and Control (JRC)*, vol. 4, no. 1, pp. 108-117, 2023.

[34] M. K. Abdelhamid, M. A. Mossa, and A. A. Hassan, "Optimizing the Dynamic Performance of a Wind Driven Standalone DFIG Using an Advanced Control Algorithm," *Journal of Robotics and Control (JRC)*, vol. 3, no. 5, pp. 633-645, 2022.

[35] L. H. Pratomo, A. F. Wibisono, and S. Riyadi, "Design and Implementation of Double Loop Control Strategy in TPFW Voltage and Current Regulated Inverter for Photovoltaic Application," *Journal of Robotics and Control (JRC)*, vol. 3, no. 2, pp. 196-204, 2022.

[36] N. M. Alyazidi, A. M. Hassanine, M. S. Mahmoud, and A. Ma'arif, "Enhanced Trajectory Tracking of 3D Overhead Crane Using Adaptive Sliding-Mode Control and Particle Swarm Optimization," *Journal of Robotics and Control (JRC)*, vol. 5, no. 1, pp. 253-262, 2024.

[37] A. Sakhi, S. E. Mansour, and A. Sekkaki, "Using learning focal point algorithm to classify emotional intelligence," *Journal of Robotics and Control (JRC)*, vol. 5, no. 1, pp. 263-270, 2024.

[38] M. Alzubi, M. Almseidin, S. Kovacs, J. Al-Sawwa, and M. Alkasassbeh, "EI-FRI: Extended incircle fuzzy rule interpolation for multidimensional antecedents, multiple fuzzy rules, and extrapolation using total weight measurement and shift ratio," *Journal of Robotics and Control (JRC)*, vol. 5, no. 1, pp. 217-227, 2024.

[39] M. N. Huynh, H. N. Duong, and V. H. Nguyen, "A passivity-based control combined with sliding mode control for a DC-DC boost power converter," *Journal of Robotics and Control (JRC)*, vol. 4, no. 6, pp. 780-790, 2023.

[40] R. Alika, E. M. Mellouli, and E. H. Tissir, "Adaptive cruise control of the autonomous vehicle based on sliding mode controller using arduino and ultrasonic sensor," *Journal of Robotics and Control (JRC)*, vol. 5, no. 1, pp. 301-311, 2024.

[41] S. E. Mansour, A. Sakhi, L. Kzaz, and A. Sekkaki, "Enhancing security mechanisms for IoT-fog networks," *Journal of Robotics and Control (JRC)*, vol. 5, no. 1, pp. 152-159, 2024.

[42] R. A. C. Leuveano, H. M. Asih, M. I. Ridho, and D. A. Darmawan, "Balancing Inventory Management: Genetic Algorithm Optimization for A Novel Dynamic Lot Sizing Model in Perishable Product Manufacturing," *Journal of Robotics and Control (JRC)*, vol. 4, no. 6, pp. 878-895, 2023.

[43] K. Yamtuan, T. Radomngam, and P. Prempraneerach, "Visual servo kinematic control of delta robot using YOLOv5 algorithm," *Journal of Robotics and Control (JRC)*, vol. 4, no. 6, pp. 818-831, 2023.

[44] M. Fuad et al., "Towards controlling mobile robot using upper human body gesture based on convolutional neural network," *Journal of Robotics and Control (JRC)*, vol. 4, no. 6, pp. 856-867, 2023.

[45] S. M. Kiran and D. N. Chandrappa, "Plant leaf disease detection using efficient image processing and machine learning algorithms," *Journal of Robotics and Control (JRC)*, vol. 4, no. 6, pp. 840-848, 2023.

[46] V. V. Kravchenko et al., "Mathematical model of a robot-spider for group control synthesis: Derivation and validation," *Journal of Robotics and Control (JRC)*, vol. 4, no. 6, pp. 849-855, 2023.

[47] M. Almaged, A. Mahmood, and Y. H. S. Alnema, "Design of an integral fuzzy logic controller for a variable-speed wind turbine model," *Journal of Robotics and Control (JRC)*, vol. 4, no. 6, pp. 762-768, 2023.

[48] Y. Mardenov, A. Adamova, T. Zhukabayeva, and M. Othman, "Enhancing Fault Detection in Wireless Sensor Networks Through Support Vector Machines: A Comprehensive Study," *Journal of Robotics and Control (JRC)*, vol. 4, no. 6, pp. 868-877, 2023.

[49] I. G. M. N. Desnanjaya, A. A. S. Pradhana, I. N. T. A. Putra, S. Widiastutik, and I. M. A. Nugraha, "Integrated room monitoring and air conditioning efficiency optimization using ESP-12E based sensors and PID control automation: a comprehensive approach," *Journal of Robotics and Control (JRC)*, vol. 4, no. 6, pp. 832-839, 2023.

[50] R. Pyla, V. Pandalaneni, and P. J. N. Raju, "Design and development of swarm AGV's alliance for search and rescue operations," *Journal of Robotics and Control (JRC)*, vol. 4, no. 6, pp. 791-807, 2023.

[51] J. Ranjith, K. Mahantesh, and C. N. Abhilash, "LW-PWECC: cryptographic framework of attack detection and secure data transmission in IoT," *Journal of Robotics and Control (JRC)*, vol. 5, no. 1, pp. 228-238, 2024.

[52] V. G. Nair, "Efficient Path Planning Algorithm for Mobile Robots Performing Floor Cleaning Like Operations," *Journal of Robotics and Control (JRC)*, vol. 5, no. 1, pp. 287-300, 2024.

[53] I. G. S. M. Diyasa, W. S. J. Saputra, A. A. N. Gunawan, D. Herawati, S. Munir, and S. Humairah, "Abnormality Determination of Spermatozoa Motility Using Gaussian Mixture Model and Matching-based Algorithm," *Journal of Robotics and Control (JRC)*, vol. 5, no. 1, pp. 103-116, 2024.

[54] D. A. N. K. Suhermanto, W. Aribowo, H. A. Shehadeh, R. Rahmadian, M. Widyartono, A. L. Wardani, and A. C. Hermawan, "Monitoring DC Motor Based on LoRa and IOT," *Journal of Robotics and Control (JRC)*, vol. 5, no. 1, pp. 54-61, 2024.

[55] A. T. Hermawan, I. A. E. Zaeni, A. P. Wibawa, G. Gunawan, W. H. Hendrawan, and Y. Kristian, "A multi representation deep learning approach for epileptic seizure detection," *Journal of Robotics and Control (JRC)*, vol. 5, no. 1, pp. 187-204, 2024.

[56] M. Afkar, R. Gavagsaz-Ghoachani, M. Phattanasak, S. Pierfederici, and W. Saksiri, "Local-stability analysis of cascaded control for a switching power converter," *Journal of Robotics and Control (JRC)*, vol. 5, no. 1, pp. 160-172, 2024.

[57] M. Fazilat and N. Zioui, "The impact of simplifications of the dynamic model on the motion of a six-jointed industrial articulated robotic arm movement," *Journal of Robotics and Control (JRC)*, vol. 5, no. 1, pp. 173-186, 2024.

[58] H. Nurwarsito, D. Suprayogo, S. P. Sakti, C. Prayogo, S. Oakley, A. P. Wibawa, and R. W. Adaby, "Development of Microclimate Data Recorder on Coffee-Pine Agroforestry Using LoRaWAN and IoT Technology," *Journal of Robotics and Control (JRC)*, vol. 5, no. 1, pp. 271-286, 2024.

[59] H. Yadavari, V. T. Aghaei, and S. I. GLU, "Addressing challenges in dynamic modeling of stewart platform using reinforcement learning-based control approach," *Journal of Robotics and Control (JRC)*, vol. 5, no. 1, pp. 117-131, 2024.

[60] R. D. Puriyanto and A. K. Mustofa, "Design and implementation of fuzzy logic for obstacle avoidance in differential drive mobile robot," *Journal of Robotics and Control (JRC)*, vol. 5, no. 1, pp. 132-141, 2024.

[61] E. Rijanto, N. Changgraini, R. P. Saputra, and Z. Abidin, "Key Factors that Negatively Affect Performance of Imitation Learning for Autonomous Driving," *Journal of Robotics and Control (JRC)*, vol. 5, no. 1, pp. 239-252, 2024.

[62] O. Y. Ismael, M. Almaged, and A. I. Abdulla, "Nonlinear model predictive control-based collision avoidance for mobile robot," *Journal of Robotics and Control (JRC)*, vol. 5, no. 1, pp. 142-151, 2024.

[63] G. S. Kumar, M. D. Kumar, S. V. R. Reddy, B. S. Kumari, and C. R. Reddy, "Injury prediction in sports using artificial intelligence applications: A brief review," *Journal of Robotics and Control (JRC)*, vol. 5, no. 1, pp. 16-26, 2024.

[64] E. Kurniawan *et al*., "A performance evaluation of repetitive and iterative learning algorithms for periodic tracking control of functional electrical stimulation system," *Journal of Robotics and Control (JRC)*, vol. 5, no. 1, pp. 205-216, 2024.

[65] I. A. Hassan, I. A. Abed, and W. A. Al-Hussaibi, "Path planning and trajectory tracking control for two-wheel mobile robot," *Journal of Robotics and Control (JRC)*, vol. 5, no. 1, pp. 1-15, 2024.

[66] D. C. E. Saputra, A. Ma'arif, and K. Sunat, "Optimizing predictive performance: Hyperparameter tuning in stacked multi-kernel support vector machine random Forest models for diabetes identification," *Journal of Robotics and Control (JRC)*, vol. 4, no. 6, pp. 896-904, 2023.

[67] A. M. Albayati, W. Chtourou, and F. Zarai, "Leveraging a two-level attention mechanism for deep face recognition with siamese one-shot learning," *Journal of Robotics and Control (JRC)*, vol. 5, no. 1, pp. 92-102, 2024.

[68] A. M. Mohan, N. Meskin, and H. Mehrjerdi, "LQG-Based Virtual Inertial Control of Islanded Microgrid Load Frequency Control and DoS Attack Vulnerability Analysis," *IEEE Access*, vol. 11, pp. 42160-42179, 2023.

[69] Y. X. Fang, Z. H. Xiao, and Z. Z. Qi, "Low-rank balanced truncation of discrete time-delay systems based on Laguerre expansions," *J. Franklin Inst.*, vol. 361, no. 6, p. 106752, 2024.

[70] C. Giamouzis, D. Garyfallou, G. Stamoulis, and N. Evmorfopoulos, "Low-rank balanced truncation of RLCk models via frequency-aware rational Krylov-based projection," in *2024 20th International Conference on Synthesis, Modeling, Analysis and Simulation Methods and Applications to Circuit Design (SMACD)*, pp. 1-4, 2024.

[71] L. Gnärig, A. Gensior, S. B. Laza, M. Carrasco, and C. Reincke-Collon, "Model reduction using singular perturbation methods for a microgrid application," in *2022 24th European Conference on Power Electronics and Applications (EPE'22 ECCE Europe)*, pp. 1-10, 2022.

[72] M. Rasheduzzaman, P. Fajri, and B. Falahati, "Balanced model order reduction techniques applied to grid-tied inverters in a microgrid," in *2022 IEEE Conference on Technologies for Sustainability (SusTech)*, pp. 195-202, 2022.

[73] T. Muhammad, A. U. Khan, M. T. Chughtai, R. A. Khan, Y. Abid, M. Islam, and S. Khan, "An adaptive hybrid control of grid tied inverter for the reduction of total harmonic distortion and improvement of robustness against grid impedance variation," *Energies*, vol. 15, no. 13, p. 4724, 2022.

[74] V. N. Kien, N. H. Trung, and N. H. Quang, "Design Low Order Robust Controller for the Generator's Rotor Angle Stabilization PSS System," *Emerging Science Journal*, vol. 5, no. 5, pp. 598-618, 2021.

[75] Q. Y. Song, U. Zulfiqar, Z. H. Xiao, M. M. Uddin, and V. Sreeram, "Balanced truncation of linear systems with quadratic outputs in limited time and frequency intervals," *arXiv preprint arXiv:2402.11445*, 2024.

[76] H. F. Sindi, S. Alghamdi, M. Y. Morgan, and A. Lasheen, "Robust LMI Controller-based Reduced Order Model for Hybrid Microgrids," in *2024 6th International Youth Conference on Radio Electronics, Electrical and Power Engineering (REEPE)*, pp. 1-5, 2024.

[77] M. H. K. Roni, Y. E. H. Emal, S. Solayman, S. J. Ritu, M. F. Rabby, M. F. Ishraque, and M. S. Rana, "Optimizing LQG controller for a single-phase power inverter in an AC microgrid system," in *2022 4th International Conference on Sustainable Technologies for Industry 4.0 (STI)*, pp. 1-5, 2022.

[78] T. Damm and M. Redmann, "Complexity reduction of large-scale stochastic systems using linear quadratic Gaussian balancing," *Journal of the Franklin Institute*, vol. 360, no. 18, pp. 14534-14552, 2023.

[79] J. König and M. A. Freitag, "Time-limited balanced truncation for data assimilation problems," *Journal of Scientific Computing*, vol. 97, no. 2, p. 47, 2023.

[80] Y. Yao, Z. Huang, and X. Du, "On the Pole Location of Reduced-order Model in Balanced Truncation Model Order Reduction," in *2023 35th Chinese Control and Decision Conference (CCDC)*, pp. 5250-5253, 2023.

[81] T. Breiten and P. Schulze, "Structure-preserving linear quadratic Gaussian balanced truncation for port-Hamiltonian descriptor systems," *Linear Algebra Appl.*, vol. 704, pp. 146–191, 2025.

[82] M. A. Rahman, M. A. Hossain, and M. M. Sikder, "A comparative study of robust optimal controllers for grid voltage control in islanded microgrids," in *2022 International Conference on Advancement in Electrical and Electronic Engineering (ICAEEE)*, pp. 1-6, 2022.

[83] T. K. Bashishtha, V. P. Singh, U. K. Yadav, and T. Varshney, "Reaction curve-assisted rule-based pid control design for islanded microgrid," *Energies*, vol. 17, no. 5, p. 1110, 2024.